

1 **Developing robust protein analysis profiles to identify bacterial acid phosphatases in**
2 **genomes and metagenomic libraries**

3

4 Zulema Udaondo^{1,2*}, Estrella Duque^{1*}, Abdelali Daddaoua³, Carlos Caselles¹, Amalia
5 Roca⁴, Paloma Pizarro-Tobias⁴, and Juan L. Ramos¹

6

7 ¹Estación Experimental del Zaidín, CSIC, E-18008 Granada, Spain

8 ²Department of Biomedical Informatics, University of Arkansas for Medical Sciences,
9 Little Rock, AR 72205, USA

10 ³Department of Biochemistry and Molecular Biology II, Faculty of Pharmacy, University
11 of Granada, Granada, Spain

12 ⁴Bio-Iliberis R&D, Peligros, Granada, Spain

13

14 *These two co-authors contributed equally to this work

15

16 Corresponding author: Juan L. Ramos

17 Contact information juanluis.ramos@eez.csic.es

18 Phone: +34 958181600 extension 289

19

20

21

22

23

24

25

26

27

28

29

30

31 ABSTRACT

32 Phylogenetic analysis of more than 4000 annotated bacterial acid phosphatases was
33 carried out. Our analysis enabled us to sort these enzymes into the following three
34 types: 1) class B acid phosphatases, which were distantly related to the other types, 2)
35 class C acid phosphatases, and 3) generic acid phosphatases (GAP). While class B
36 phosphatases are found in a limited number of bacterial families, which include known
37 pathogens, class C acid phosphatases and GAP proteins are found in a variety of
38 microbes that inhabit soil, fresh water and marine environments. As part of our analysis
39 we developed three profiles, named Pfr-B-Phos, Pfr-C-Phos and Pfr-GAP, to describe the
40 three groups of acid phosphatases. These sequence-based profiles were then used to
41 scan genomes and metagenomes to identify a large number of formerly unknown acid
42 phosphatases. A number of proteins in databases annotated as hypothetical proteins
43 were also identified by these profiles as putative acid phosphatases. To validate these
44 *in silico* results, we cloned genes encoding candidate acid phosphatases from genomic
45 DNA, or recovered from metagenomic libraries or genes synthesized *in vitro* based on
46 protein sequences recovered from metagenomic data. Expression of a number of these
47 genes, followed by enzymatic analysis of the proteins, further confirmed that sequence
48 similarity searches using our profiles could successfully identify previously unknown acid
49 phosphatases.

50

51

52 **INTRODUCTION**

53 Phosphorous is a major component of cells in all living organisms and all prokaryotic and
54 eukaryotic cells have developed mechanisms for the uptake of inorganic phosphate,
55 which is used in the biosynthesis of phospholipids, sugar phosphates, nucleotides and
56 other molecules (Barea and Richardson, 2015). Despite phosphorous being one of the
57 most abundant non-metallic elements in the earth's crust, it is frequently found in forms
58 that are not bioavailable - a reality that often leads to phosphorous nutrient limitation
59 (Ågren *et al.*, 2012; Sosa *et al.*, 2019). Inorganic phosphorous forms are often solubilized
60 by plants and microorganisms (bacteria and fungi) through the production of weak acids

61 (Barea and Richardson, 2015). However, a number of common organic phosphorous
62 compounds (i.e., phytic acid, sugar phosphates, nucleotides, phospholipids and others)
63 must be first hydrolysed by phosphatases to yield inorganic phosphate, which can
64 subsequently be taken up by microorganisms and plants to be used as a phosphorous
65 source (Hayes *et al.*, 2000; Alori *et al.*, 2017; Thomashow *et al.*, 2018). Evidence suggests
66 that phosphatase activity in soils and aquatic environments is of ecological relevance
67 and is a driver of the productivity of terrestrial ecosystems (Turner *et al.*, 2013; Margalef
68 *et al.*, 2017) and influence primary and secondary production in fresh waters and marine
69 environments (Martiny *et al.*, 2019).

70 There are two types of phosphatases among the phosphoric ester hydrolases which are
71 defined based on their optimal pH. Alkaline phosphatases are a broad group of well
72 characterized enzymes that use different mechanisms and co-factors to carry out their
73 function (Mullaney and Ullah, 2003; Ragot *et al.*, 2015; Lidbury *et al.*, 2017; Neal *et al.*,
74 2018). Acid phosphatases are, in general, non-specific phosphatases with broad
75 substrate specificity and are often secreted across the outer membrane or are located
76 in the periplasmic space (Thaller *et al.*, 1997). At least three different types of
77 prokaryotic phosphatases that function at acidic pH have been distinguished mainly
78 based on their sequences; they are known as types A, B and C (Thaller *et al.*, 1997;
79 Lidbury *et al.*, 2017; Neal *et al.*, 2018). It was noted that the B class phosphatases are
80 generally associated with pathogenic microbes while the other types are widely
81 distributed in nature (Neal *et al.*, 2018). While the importance of acid phosphatases to
82 the acquisition of phosphorous in soils, fresh waters and marine environments (Neal *et al.*
83 *et al.*, 2018); Margalef *et al.* (2017) compiled phosphatase activities from a large number
84 studies of natural ecosystems and made 329 observations for acid phosphatases versus
85 72 for alkaline phosphatases, highlighting the environmental importance of acid
86 phosphatases.

87 The work described here aims to contribute further to the understanding of organic
88 phosphorous mobilisation in the environment by acid phosphatases. To this end we
89 developed three robust profiles that can unequivocally identify the different types of
90 acid phosphatase types. We have empirically validated the profiles by cloning and

91 expression of putative acid phosphatases rescued from genomes, or recovered from
92 functional metagenomic libraries or genes synthesized *in vitro* based on protein
93 sequences recovered from metagenomic libraries (Fierer *et al.*, 2013; Berini *et al.*, 2017;
94 Duque *et al.*, 2018). This profiling methodology will serve as a valuable resource for the
95 identification of these important enzymes within the preponderance of already
96 sequenced genomes and widely available metagenomic data. Furthermore, this study
97 provides a proof-of-concept for the successful use of profiles to characterize enzymes
98 involved in biogenic cycles.

99

100 **RESULTS AND DISCUSSION**

101 As a first step towards the identification of bacterial acid phosphatases we retrieved
102 4644 sequences annotated as bacterial acid phosphatases (either due to protein name
103 or Pfam domain composition) from the Uniprot Database (UniProt: a worldwide hub of
104 protein knowledge, 2019). A phylogenetic tree was constructed with a refined set of
105 3741 protein sequences (see Experimental Procedures) and the results are shown in
106 Figure 1. The bacterial acid phosphatase tree has, as expected, three clear branches; one
107 represented by the outer blue circle which corresponds to class B (Figure 1), another
108 represented by the outer purple circle that corresponds to class C and the other
109 represented by the outer green circle that corresponds to Generic Acid Phosphatases
110 class A (GAP) (Figure 1). Supplementary Table 1 contains information collected from the
111 Uniprot database for each of the refined datasets of acid phosphatases. The
112 phylogenetic tree from Supplementary Figure 1 shows that acid phosphatases from class
113 GAP, B and C belong to three well defined monophyletic groups. The unrooted tree also
114 revealed that sequences from class A and C are closest relatives and therefore
115 sequences from class B are from an evolutionary point of view more distant from the
116 other two.

117 The blue branch of the tree grouped 512 sequences that corresponded with annotated
118 acid phosphatases of class B, the purple branch included 1701 sequences of annotated
119 class C acid phosphatases; while the other set, which we named GAP, comprised 1528
120 non-specific class A acid phosphatases. The analysis of the sequences at the family level

121 showed that class C and GAP proteins were found widely distributed among microbes
122 that inhabit soils, fresh water and marine environments. In contrast, class B acid
123 phosphatases are present in a limited number of microbial families which include
124 Enterobacteriaceae, Pasteurellaceae, Morganellaceae, Aeromonadaceae and
125 Vibrionaceae (Figure 1 and 2), of which some are pathogens (supplementary Table 2A,
126 2B, 2C). Conversely, it should be noted that class C and GAP acid phosphatases were also
127 present in some Enterobacteriaceae. For example, in *Salmonella* and *Klebsiella* genomes
128 GAP proteins were identified and in a number of *Enterobacter* species (mainly *cloacae*)
129 class C proteins were found. In contrast in the *Escherichia coli* species, despite being a
130 broad taxonomic group (Abram *et al.*, 2020), only class B acid phosphatases were
131 identified (supplementary Table 2).

132 Bacterial acid phosphatases have previously been identified through a number of
133 signatures; for example, the database of families and domain proteins PROSITE (Sigrist
134 *et al.*, 2002) identified bacterial acid phosphatase sequences based on short sequence
135 pattern motifs defined by the signature PS01157 (pattern G-S-Y-P-S-G-H-T). The
136 compendium of protein fingerprints *PRINTS* database (Attwood *et al.*, 2000), contains
137 the signature PR00483 which corresponds to a 5-element fingerprint from bacterial acid
138 phosphatases derived from an initial alignment of a limited number of sequences. Four
139 profiles were available from TIGRFAM database that were constructed using a limited
140 set of acid phosphatase sequences (TIGR03397, 01675, 01672 and 01668); however,
141 these profiles were found to have no discriminatory power. Other databases, such as
142 Pfam domain protein database (El-Gebali *et al.*, 2019) and Simple Modular Architecture
143 Research Tool (SMART) (Letunic and Bork, 2018) contain a number of entries related to
144 identification and classification of bacterial acid phosphatases. Nonetheless, none of the
145 above motifs and classifications distinguish unequivocally between the three classes of
146 bacterial acid phosphatases.

147 To establish a new criterion defining the three kinds of acid phosphatases represented
148 in the phylogenetic tree, we decided to explore the construction of PROSITE generalized
149 profiles, which are not available in the PROSITE database (<https://prosite.expasy.org>).
150 Profiles are weight matrices that are useful for grouping proteins into families (Gromiha,

151 2010) and use quantitative motif descriptors which are given as linear sequences that
152 comprise weighted match or mismatch residues and insert sequences in a profile
153 position (Sigrist *et al.*, 2002). Given that the phylogenetic tree defined three branches,
154 according to differences in their amino acid sequences, we expected that a Profile for
155 each of the branches would result in a net gain in specificity for identification and
156 assignation of the entire collection of bacterial acid phosphatases.

157 To construct the three new profiles, we proceeded as suggested by PROSITE
158 (https://prosite.expasy.org/prosuser.html#meth_prf). To create these profiles, we used
159 the three sets of proteins identified in each of the branches of the tree, the profile for
160 class B phosphatases (Prf-B-Phos) was constructed using a set of 512 seed sequences,
161 for the profile for class C we used 1701 sequences while for the profile for GAP (Pfr-
162 GAP), due to the high variability in the sequence similarity and sequence length from
163 members of this class, we used a filtered set of 948 out of the 1528 sequences from the
164 previous analysis (supplementary Tables 3A, 3B and 3C). The three profiles obtained in
165 this study are publicly available in supplementary Table 4. The generation of a profile
166 requires a multiple-alignment of the seed sequences as input, which was performed
167 using Muscle (Edgar, 2004). The consensus sequences derived from the multiple-
168 alignments (supplementary Tables 3A, 3B and 3C) showed conserved regions with high-
169 sequence identity scattered throughout the full sequence of the proteins. This reflects
170 the existence of several functional constraint regions, with lower site-specific
171 substitution ratio distributed along the protein sequences belonging to each of the
172 classes. This is in contrast with most sequence patterns where high-sequence identity
173 regions are restricted to active sites, cofactor binding domains or specific DNA binding
174 regions (Fuglebakk *et al.*, 2012).

175 The multiple-alignment revealed that the short patterns used previously to define these
176 acid phosphatases were in a wider sequence identity context and this warranted the
177 construction of profiles to encompass the full gamut of acid phosphatase sequences
178 belonging to these families. We used the script *pfmake* to translate the multiple-
179 alignment into a matrix table of positions and convert frequency distributions into
180 positive specific amino acid weights and gaps according to the original algorithms of

181 Sibbald and Argos (Sibbald and Argos, 1990) and Gribskov *et al* (1987). Once the profiles
182 were constructed we proceeded to calibrate and validate the profiles as recommended
183 by PROSITE (described in Experimental Procedures), for this the profiles were run against
184 a database to produce a list of sorted scores. It has been previously empirically
185 determined that cut-off values of Z-scores equal or greater than 8.5 are biologically
186 significant and warrant the correct assignment of a protein to a family (Gallegos *et al.*,
187 1997; Sigrist *et al.*, 2002; Godoy *et al.*, 2010).

188 As a proof of concept, the three profiles were used as input for *pfsearch* v2.3 from the
189 PTOOLS suite to scan the complete set of Uniref100 proteins (downloaded from the
190 UniProt database on May 24, 2019). As a result, 6000 proteins were matched with Pfr-
191 GAP (Figure 3 and Supplementary Figure 2), 2132 protein sequences were matched by
192 the Pfr-B-Phos (Figure 3 and Supplementary Figure 3) and 10494 with Pfr-C-Phos (Figure
193 3 and Supplementary Figure 4).

194 We found that Pfr-B-Phos identified acid phosphatases preferentially from
195 enterobacteria, vibrios and other microorganisms mainly from orders Pasteurellales and
196 Bacillales (see Supplementary Figure 3) whose life style indicated a close relationship
197 with eukaryotes, as mentioned above, and confirming previous studies (Gandhi and
198 Chandra, 2012; Neal *et al.*, 2018). Conversely, we found that Pfr-C-Phos and Pfr-GAP
199 identified acid phosphatases from a variety of different sources in a highly-specific and
200 sensitive manner, including Acidobacteria, Actinobacteria, alpha, beta, gamma and
201 epsilon proteobacteria, Firmicutes, Verrumicrobia, and Bacterioidetes among many
202 others (see supplementary Figure 2, and supplementary Figure 4). The results obtained
203 with the three profiles against Uniref100 database (Suzek *et al.*, 2015) demonstrated the
204 ability of Pfr-GAP, Pfr-C-Phos and Pfr-B-Phos to discriminate between all classes of acid
205 phosphatases displayed in the phylogenetic tree and within a wide taxonomic range. It
206 is worth noting that although the three profiles were developed using only bacterial
207 sequences, presumed eukaryotic acid phosphatases were also found in all cases. The
208 complete set of raw hits sorted by output score is shown in supplementary Table 5.
209 Remarkably, although these are non-filtered results, the high accuracy of the three
210 profiles allowed the identification of proteins belonging to each of the classes at very

211 low score numbers. The specificity of the profiles also identified a large number of
212 putative acid phosphatase sequences which were annotated in the Uniref100 database
213 as “uncharacterized protein”.

214 To further validate the new profiles, we decided to test if Pfr-GAP, Pfr-C-Phos, and Pfr-
215 B-Phos could identify acid phosphatases within available annotated whole genomes, in
216 metagenomic libraries in which proteins are annotated as Hypothetical Proteins of
217 unknown function, as well as proteins recovered from functional metagenomic libraries
218 after screening for positive phosphatase activity. We found that the Pfr-GAP, Pfr-C-Phos
219 and Pfr-B-Phos profiles could indeed identify a number of potential acid phosphatases
220 in all of these screens. Specifically, we found that in the annotated reference genomes
221 collected from the NCBI database 4649 proteins were identified by the Pfr-A GAP profile,
222 862 by the Pfr-C-Phos profile and 128 proteins by the Pfr-B-phos profile (Figure 3). For
223 most type strains the number of GAP acid phosphatases and class C was between 1 and
224 3, although we found 13 genomes with 6 GAP acid phosphatases and 2 genomes with
225 up to 5 class C acid phosphatase. In those genomes in which an acid phosphatase of class
226 B was present, a single gene was always found, except in one case in which a duplication
227 was identified, and another genome which bore 4 class B acid phosphatase genes. As
228 validation of the proof of concept, we rescued acid phosphatases from the genomes of
229 two microorganisms (i.e., *Pyrococcus*, and *Bacillus subtilis* strain 168). A search using the
230 three profiles with *pfsearch* against the genomes of *Pyrococcus furiosus* DSM 3638, and
231 *Bacillus subtilis* str. 168 identified the protein sequences PF0040 and BSU_36530 as
232 putative GAP acid phosphatases, encoded in each genome respectively. *Bacillus subtilis*
233 BSU_36530 was previously annotated as undecaprenyl diphosphatase, while PF0040
234 from *P. furiosus* was annotated as an acidic acid phosphatase. To confirm these ‘hits’
235 empirically, we used whole chromosomal DNA from these microorganisms and cloned
236 the amplified DNA into pET28 as described in Experimental Procedures (Table 1).

237 As an initial step for confirmation of phosphatase activity, we spread the cells on LB
238 medium supplemented with BCIP and found that colonies turned deep blue, suggesting
239 that the cloned genes encoded, as expected, phosphatases. A single random clone
240 bearing the gene from each of the two microorganisms was kept. Then, cells were grown

241 in liquid LB and acid phosphatase activity determined over a wide pH range in
242 permeabilised cells as described in Experimental Procedures. The results revealed that
243 the optimal pH was in the range of 5 to 6 (Table 2).

244 Our laboratory previously screened a functional metagenomic library from
245 hydrocarbon-polluted soil after land farming and identified a clone, named FOS M2-62,
246 that had robust phosphatase activity (see Experimental Procedures). The fosmid of this
247 clone was sequenced and our profiles were used to identify it as a putative GAP acid
248 phosphatase. We subsequently cloned it into pET28 to generate pET28_FOS M2-62.

249 Phosphatase assays revealed that the AP-M2-62 protein had high activity between pH 5
250 and pH 7 (Table 2), but lower activity at pH greater than 7 or lower than 5. This suggests
251 that AP-M2-62 is indeed an acid phosphatase.

252 We then explored the ability of our constructed profiles to identify hypothetical proteins
253 as putative acid phosphatase from metagenomic libraries. To this end we screened
254 1,552,866 hypothetical proteins from soil metagenomes and 4,925,568 sequences from
255 marine metagenomes (downloaded in June 2019 from the NCBI database) and we found
256 that the search yielded a total of 539 hypothetical proteins from the soil metagenome
257 and 351 hypothetical proteins from marine metagenomes using Pfr-GAP profile
258 (Supplementary Table 5). The Pfr-C-Phos profile was able to find 242 proteins from
259 marine metagenomes and 23 from terrestrial metagenomes. The Pfr-B-Phos profile was
260 able to find only 11 proteins from marine metagenomes. These results are in line with
261 the initial phylogenetic tree results in the sense that class B proteins are poorly
262 represented in marine and terrestrial ecosystems.

263 This data confirmed that among non-characterized acid phosphatases, generic acid
264 phosphatases and class C phosphatases were more abundant than class B, and that class
265 C and GAP can be considered cosmopolitan proteins as they can be found in a wide range
266 of niches. We found that among the set of non-characterized proteins 1 acid
267 phosphatase could be rescued per 3,000 sequences in soil metagenomes while 1 acid
268 phosphatase protein was found every 14,000 sequences in marine metagenomes.
269 Because the quality of metagenomic sequences is non-homogeneous and because our

270 data are raw hit counts, at present we cannot make any conclusions regarding the
271 biogeographic distribution of acid phosphatases based on metagenomic data.

272 Considering the apparent abundance of these sequences, we explored whether the
273 identified sequences were indeed acid phosphatases. To this end we choose two
274 sequences with the highest Z-score from each acid phosphatase family (Supplementary
275 Table 6) and synthesised the corresponding genes. We then cloned and expressed them
276 in *Escherichia coli* and enzyme activity was determined in permeabilised whole cells
277 using the Britton-Robinson poly-buffer. We found that the six metagenomic acid
278 phosphatase had optimal activity at acidic pH (Table 2 and supplementary Table 7).
279 These results further validate the ability of the profiles to find acid phosphatase enzymes
280 from metagenomes. It is worth mentioning that although the MET_A1 enzyme exhibited
281 the highest activity at pH 5.5 to 6, it had significant activity pH in the pH range between
282 5 and 9 (Table 2).

283 In order to further characterize in more detail, the kinetics properties of the
284 metagenomic acid phosphatases, we purified three proteins (see Experimental
285 Procedures) and the kinetics parameters determined using isothermal titration
286 calorimetry (ITC) (Watt, 1990; Williams and Toone, 1993). The initial rate of reaction (V_o)
287 with different concentrations of pNPP was determined from the slope of the linear
288 portion of the curve of integrated heats versus time as described by Bianconi (2003). We
289 found that values for V_o followed typical Michaelis-Menten kinetics and K_{cat} and K_M were
290 calculated by fitting the curve to the Michaelis-Menten kinetics equation using non-
291 linear regression (Ababou and Ladbury, 2006). For MET_A_1, M2-F62, and MET_C_1,
292 values of K_M were $49.3 \pm 2.6 \mu\text{M}$, $29.7 \pm 0.02 \mu\text{M}$ and $23.8 \pm 6.9 \mu\text{M}$, respectively; and
293 k_{cat} were 0.63 s^{-1} , 0.55 s^{-1} , and 0.26 s^{-1} , respectively. Our results revealed that the
294 substrate affinities were in the low micromolar range with up to 2-fold differences; k_{cat}
295 values differed by up to 2.5-fold. The K_M values we determined are lower than those
296 measured for acid phosphatases from different sources using classical
297 spectrophotometric assays (Reilly *et al.*, 2009; Zhang *et al.*, 2013; Wang *et al.*, 2018).

298
299

300 **CONCLUSIONS**

301 In conclusion, we have constructed a phylogenetic tree for acid phosphatases that
302 grouped them into three branches. For each of the branches a Prosite profile was
303 constructed and validated; the three profiles were shown to be effective in the
304 differentiation of the three sets of acid phosphatases. These profiles were able to assign
305 a set of proteins annotated as hypothetical proteins in databases as being acid
306 phosphatases (Suppl. Table 4). We tested our 'hits' empirically and confirmed
307 phosphatase activity at acidic pH. Use of these profiles and the underlying strategy could
308 serve as a powerful approach to explore the role that acid phosphatases play in primary
309 productivity in edaphic and aquatic environments.

310

311

312 **EXPERIMENTAL PROCEDURES**

313

314 ***Phylogenetic tree construction***

315 Sequences were downloaded from the Uniprot database by filtering proteins that
316 belong to the Domain = bacteria and the annotation = acid phosphatase and 5'
317 nucleotidase lipoprotein ep4 family; the later corresponds to class C acid phosphatases.
318 Using these filters (on April 26, 2019) we retrieved 4644 protein sequences. Muscle
319 v3.8.1551 (Edgar, 2004) alignment software with parameter - maxiters 1000 was used
320 to align the set of 4644 protein sequences and construct the phylogenetic tree. Very
321 divergent sequences were filtered and removed from the alignment until a final set of
322 3741 amino acid sequences were kept. The final set of sequences was aligned again
323 using Muscle v3.8.1551 with the same parameters. Aligned sequences were used as
324 input for the IQ-TREE software v1.6.10 (Nguyen *et al.*, 2015) with parameters -nt AUTO,
325 -bb 1000 -m TESTMERGE. The maximum likelihood tree was constructed following the
326 model of evolution WAG with parameters F+R10 (IQ-TREE uses ModelFinder).
327 Phylogenetic trees were plotted using the Interactive Tree of Life (iTOL) suite software
328 v4 (Letunic and Bork, 2016).

329

330 **Profile construction**

331 To construct PROSITE “generalized” profiles, first we established the “seed protein
332 sequences” that would determine the sensitivity and average quality of the profiles.

333 Once visualized, the phylogenetic tree branches annotated as class B phosphatases,
334 class C and generic acid phosphatases were aligned separately and filtered according to
335 observed divergences in the alignment. Then *pfw* and *pfmake* scripts from PFTOOLS v2.3
336 (Gribskov *et al.*, 1987; Sigrist *et al.*, 2002; Bucher *et al.*, 2015) were used to compute
337 new weights for each individual sequence from the multiple sequence alignment and to
338 construct the profile respectively. The matrix BLOSUM 45 was selected for the
339 construction of the profile.

340 *Pfsearch* and *pfscan* were used to calibrate each profile against a calibration database.
341 The calibration database was made from the entire collection of Swiss-Prot protein
342 sequences filtered by Taxonomy = bacteria. The database contained a total of 334,009
343 sequences that were shuffled randomly with a sliding window of 20 residues using the
344 script *fasta-shuffle-letters* from MEME suite v5.0.2 (Bailey *et al.*, 2015).

345 Searches with the three profiles using Uniref100 database, a local database of
346 representative bacterial and archaea sequences and hypothetical protein databases
347 from metagenomic samples, were all done using *pfscan* script from PFTOOLS v2.3 with
348 parameters *-z -f* (Bucher *et al.*, 2013).

349

350 **Sequences in databases**

351 Uniref100 database was downloaded to be used locally in May, 2019. The set of protein
352 FASTA sequences from representative strains was downloaded from the NCBI database
353 in August, 2019. The set of representative strains was obtained via genome browse from
354 NCBI <https://www.ncbi.nlm.nih.gov/genome/browse#!/overview/> and then filtered by
355 “archaea” AND “bacteria” AND “representative genome”. The two sets of hypothetical
356 proteins used in these analyses were obtained from NCBI protein database using filters:
357 “soil metagenome” AND “hypothetical protein” and “marine metagenome” AND
358 “hypothetical protein”

359

360 **Construction of a functional soil metagenomic library**

361 Soil samples were taken from hydrocarbon polluted soil after land farming. High-
362 molecular-weight DNA extraction was performed from the soil using the commercial
363 GNOME DNA kit (MP, Biomedicals) according to the manufacturer's instructions. DNA
364 fragments of approximately 40 kb were recovered and ligated into the pCC1FOS vector
365 (Epicentre®), and the product was transduced into *E. coli* EPI300 (Raleigh *et al.*, 2002)
366 according to the manufacturer's protocol. Screening for phosphatase activity was
367 performed by replicating the metagenomic library onto agar LB plates with 40 mg per
368 mL of 5-bromo-4-chloro-3-indolyl phosphate (BCIP Applichem, Darmstadt, Germany) as
369 substrate, supplemented with 12.5 µg per mL chloramphenicol and 0.01% L-arabinose.
370 Following replication, the colonies were incubated for 24 h at 37°C. A total of 64 clones
371 with phosphatase activity were identified and detected as pale to dark blue colonies. A
372 single clone, named M2-62, that turned deep blue on these plates was used for further
373 analysis in this study.

374

375 **Cloning of putative acid phosphatases in Escherichia coli.**

376 DNA from *Pyrococcus furiosus* DSM 3638 and *Bacillus subtilis* DSM 204 were obtained
377 from the DSMZ culture collection. The *Bacillus subtilis* gene was PCR amplified with the
378 following primers 5'-TTGAACTACGAAATTTTAAAGCAATCC-3' and 5'-
379 TTCTTAGAAATTTTGATCGGTTGG-3', while the *Pyrococcus* gene was amplified using the
380 following pair of primers 5'-ATGCTGGCAATACTTACGGCAA-3' and 5'-
381 TCACTTATCCACTTTAAAAAAGATGCGC-3'; amplified DNA was subsequently cloned into
382 pTOPO and further subcloned into pET28 after digestion with NdeI and EcoRI. Plasmids
383 were transformed into *E. coli* BL21 (DE3) (Studier *et al.*, 2009). For amplification of the
384 open reading frame encoding the AP-M2-62 protein, fosmid DNA was prepared and the
385 following primers: 5'-CATATGAAAAAATACCTGAACCCTTC-3' (forward) and 5'-
386 GGATCCTCAGTGCTGGGTCAG-3' (reverse) were used. Following PCR amplification,
387 under standard conditions, the fragment was cloned into the pMBL vector to yield
388 pMBL_FOSM2-62. The plasmid was subsequently digested with NdeI/BamHI and the

389 806 bp fragment bearing the ORF AP-M2-62 was cloned into pET28b (+) digested with
390 the same enzymes (Table 1).

391

392 ***Cloning of putative metagenomic acid phosphatases in Escherichia coli***

393 Protein sequences retrieved from metagenomic libraries with a high Z-score for GAP,
394 class B and class C were manually curated. The protein sequences were then translated
395 into DNA sequences with optimized codon usage for *E. coli*, synthesized in vitro by
396 Genescript, cloned into pET28 and expressed from the P_{lac} .

397

398 ***Growth of Escherichia coli and in vivo acid phosphatase activity.*** *Escherichia coli* BL21

399 (DE3) transformed with the corresponding plasmid was grown in 100 mL conical flasks
400 containing 25 mL of LB supplemented with 0.025 mg/mL kanamycin (pET28). Cultures
401 were incubated at 37 °C with shaking until they reached a turbidity at 660 nm (OD_{660}) of
402 0.6, at which point 0.1 mM isopropyl- β -D-thiogalactopyranoside (IPTG) was added, to
403 induce expression, incubation was continued overnight. After growth of *E. coli* the
404 turbidity of the cultures was adjusted to 1 in 600 μ L of lysis buffer (100 mM acetate, pH
405 5.5, $CaCl_2$, 1 mM, and Tween 80, 0.01% (or a drop of toluene) (Lassen *et al.*, 2001). The
406 assay was performed by combining 100 μ L of permeabilized cells with 10 μ L of a solution
407 of 100 mM *p*-nitrophenyl phosphate (pNPP) dissolved in 0.1 M Na-acetate buffer, pH
408 5.5. The reaction mixture was incubated for 30 min at 25°C. Subsequently, 100 μ L of 0.5
409 M sodium hydroxide in water was added to stop the reaction. The samples were then
410 centrifuged in a bench centrifuge (5 min at 10000 rpm) and the absorbance at 405 nm
411 was measured in a spectrophotometer. To determine the optimal pH range the Britton-
412 Robinson poly-buffer (40 mM boric acid, 40 mM acetic acid and 40 mM phosphoric acid)
413 was adjusted with NaOH to a pH between 2 and 9 (Souri *et al.*, 2013). Other conditions
414 for the acid phosphatase assays are those mentioned above.

415

416 ***Protein purification.***

417 For protein purification, cells were suspended in 25 mL of buffer A (50 mM Hepes pH
418 6.9; 300 mM NaCl; 1 mM dithiothreitol) with EDTA-free protease inhibitor mixture. Cells

419 were lysed by two passes through a French Press at a p.s.i. of 1000. The cell suspension
420 was then centrifuged at 20,000 x g for 1 hour. The pellet was discarded and the
421 supernatant was filtered and loaded onto a 5 mL His-Trap chelating column (GE
422 Healthcare, St. Gibes, UK). The proteins were eluted with a 10 to 500 mM gradient of
423 imidazol in buffer A. The purity of the eluate was determined by running 12% SDS-PAGE
424 gels. Homogenous protein preparations were dialyzed overnight against buffer A but
425 supplemented with 10% [v/v] glycerol). Dialyzed protein was collected at a
426 concentration of about 1 mg/mL and stored in 1 mL aliquots at -80 °C.

427

428

429 **Acknowledgments.** Work in Granada was supported by grant RTI2018-094370-B-I00, at
430 CSIC and grant EC-H2020-685474 at Bio-Iliberis R&D. Part of the data analysed in this
431 work was performed on the High-Performance Computing Facilities, in particular the
432 Grace cluster, provided by the University of Arkansas for Medical Sciences (UAMS),
433 managed by the Department of Biomedical Informatics. We thank Ben Pakuts for critical
434 reading of the manuscript.

435

436 CONFLICT OF INTEREST:

437 The authors declare no conflict of interest

438

439 **References**

440

Ababou, A. and Ladbury, J.E. (2006) Survey of the year 2004: literature on applications
of isothermal titration calorimetry. *Journal of Molecular Recognition* **19**: 79–89.

Abram, K., Udaondo, Z., Bleker, C., Wanchai, V., Wassenaar, T.M., Robeson, M.S., and
Ussery, D.W. (2020) What can we learn from over 100,000 Escherichia coli
genomes? *bioRxiv* 708131.

- Ågren, G.I., Wetterstedt, J.Å.M., and Billberger, M.F.K. (2012) Nutrient limitation on terrestrial plant growth – modeling the interaction between nitrogen and phosphorus. *New Phytologist* 953–960.
- Alori, E.T., Glick, B.R., and Babalola, O.O. (2017) Microbial Phosphorus Solubilization and Its Potential for Use in Sustainable Agriculture. *Front Microbiol* 8:.
- Attwood, T.K., Croning, M.D.R., Flower, D.R., Lewis, A.P., Mabey, J.E., Scordis, P., et al. (2000) PRINTS-S: the database formerly known as PRINTS. *Nucleic Acids Res* 28: 225–227.
- Bailey, T.L., Johnson, J., Grant, C.E., and Noble, W.S. (2015) The MEME Suite. *Nucleic Acids Res* 43: W39–W49.
- Barea, J.-M. and Richardson, A.E. (2015) Phosphate Mobilisation by Soil Microorganisms. In *Principles of Plant-Microbe Interactions: Microbes for Sustainable Agriculture*. Lugtenberg, B. (ed). Cham: Springer International Publishing, pp. 225–234.
- Berini, F., Casciello, C., Marcone, G.L., and Marinelli, F. (2017) Metagenomics: novel enzymes from non-culturable microbes. *FEMS Microbiol Lett* 364.
- Bianconi, M.L. (2003) Calorimetric Determination of Thermodynamic Parameters of Reaction Reveals Different Enthalpic Compensations of the Yeast Hexokinase Isozymes. *J Biol Chem* 278: 18709–18713.
- Bucher, P., Cerutti, L., Pagni, M., and Schuepbach, T. (2013) PfTools Software Suite.
- Bucher, P., Karplus, K., Moeri, N., and Hofmann, K. (2015) A Flexible Motif Search Technique Based on Generalized Profiles. *Computers and Chemistry* 20: 3–24.
- Duque, E., Daddaoua, A., Cordero, B.F., Udaondo, Z., Molina-Santiago, C., Roca, A., et al. (2018) Ruminant metagenomic libraries as a source of relevant hemicellulolytic enzymes for biofuel production. *Microbial Biotechnology* 11: 781–787.
- Edgar, R.C. (2004) MUSCLE: multiple sequence alignment with high accuracy and high throughput. *Nucleic Acids Res* 32: 1792–1797.

- El-Gebali, S., Mistry, J., Bateman, A., Eddy, S.R., Luciani, A., Potter, S.C., et al. (2019) The Pfam protein families database in 2019. *Nucleic Acids Res* **47**: D427–D432.
- Fierer, N., Ladau, J., Clemente, J.C., Leff, J.W., Owens, S.M., Pollard, K.S., et al. (2013) Reconstructing the Microbial Diversity and Function of Pre-Agricultural Tallgrass Prairie Soils in the United States. *Science* **342**: 621–624.
- Fuglebakk, E., Echave, J., and Reuter, N. (2012) Measuring and comparing structural fluctuation patterns in large protein datasets. *Bioinformatics* **28**: 2431–2440.
- Gallegos, M.T., Schleif, R., Bairoch, A., Hofmann, K., and Ramos, J.L. (1997) Arac/XylS family of transcriptional regulators. *Microbiol Mol Biol Rev* **61**: 393–410.
- Godoy, P., Molina-Henares, A.J., Torre, J.D.L., Duque, E., and Ramos, J.L. (2010) Characterization of the RND family of multidrug efflux pumps: in silico to in vivo confirmation of four functionally distinct subgroups. *Microbial Biotechnology* **3**: 691–700.
- Gribkov, M., McLachlan, A.D., and Eisenberg, D. (1987) Profile analysis: detection of distantly related proteins. *PNAS* **84**: 4355–4358.
- Gromiha, M.M. (2010) Protein bioinformatics: from sequence to function, Academic Press.
- Hayes, J.E., Richardson, A.E., and Simpson, R.J. (2000) Components of organic phosphorus in soil extracts that are hydrolysed by phytase and acid phosphatase. *Biol Fertil Soils* **32**: 279–286.
- Lassen, S.F., Breinholt, J., Østergaard, P.R., Brugger, R., Bischoff, A., Wyss, M., and Fuglsang, C.C. (2001) Expression, Gene Cloning, and Characterization of Five Novel Phytases from Four Basidiomycete Fungi: *Peniophora lycii*, *Agrocybe pediades*, a *Ceriporia* sp., and *Trametes pubescens*. *Appl Environ Microbiol* **67**: 4701–4707.
- Letunic, I. and Bork, P. (2018) 20 years of the SMART protein domain annotation resource. *Nucleic Acids Res* **46**: D493–D496.

- Letunic, I. and Bork, P. (2016) Interactive tree of life (iTOL) v3: an online tool for the display and annotation of phylogenetic and other trees. *Nucleic Acids Res* **44**: W242–W245.
- Lidbury, I.D.E.A., Fraser, T., Murphy, A.R.J., Scanlan, D.J., Bending, G.D., Jones, A.M.E., et al. (2017) The ‘known’ genetic potential for microbial communities to degrade organic phosphorus is reduced in low-pH soils. *MicrobiologyOpen* **6**: e00474.
- Margalef, O., Sardans, J., Fernández-Martínez, M., Molowny-Horas, R., Janssens, I.A., Ciais, P., et al. (2017) Global patterns of phosphatase activity in natural soils. *Sci Rep* **7**: 1–13.
- Martiny, A.C., Lomas, M.W., Fu, W., Boyd, P.W., Chen, Y.L., Cutter, G.A., et al. (2019) Biogeochemical controls of surface ocean phosphate. *Science Advances* **5**: eaax0341.
- Mullaney, E.J. and Ullah, A.H.J. (2003) The term phytase comprises several different classes of enzymes. *Biochemical and Biophysical Research Communications* **312**: 179–184.
- Neal, A.L., Blackwell, M., Akkari, E., Guyomar, C., Clark, I., and Hirsch, P.R. (2018) Phylogenetic distribution, biogeography and the effects of land management upon bacterial non-specific Acid phosphatase Gene diversity and abundance. *Plant Soil* **427**: 175–189.
- Nguyen, L.-T., Schmidt, H.A., von Haeseler, A., and Minh, B.Q. (2015) IQ-TREE: A Fast and Effective Stochastic Algorithm for Estimating Maximum-Likelihood Phylogenies. *Mol Biol Evol* **32**: 268–274.
- Ragot, S.A., Kertesz, M.A., and Bünemann, E.K. (2015) *phoD* Alkaline Phosphatase Gene Diversity in Soil. *Appl Environ Microbiol* **81**: 7281–7289.
- Raleigh, E.A., Elbing, K., and Brent, R. (2002) Selected Topics from Classical Bacterial Genetics. *Current Protocols in Molecular Biology* **59**: 1.4.1-1.4.14.

- Reilly, T.J., Chance, D.L., Calcutt, M.J., Tanner, J.J., Felts, R.L., Waller, S.C., et al. (2009) Characterization of a Unique Class C Acid Phosphatase from *Clostridium perfringens*. *Appl Environ Microbiol* **75**: 3745–3754.
- Sibbald, P.R. and Argos, P. (1990) Weighting aligned protein or nucleic acid sequences to correct for unequal representation. *J Mol Biol* **216**: 813–818.
- Sigrist, C.J.A., Cerutti, L., Hulo, N., Gattiker, A., Falquet, L., Pagni, M., et al. (2002) PROSITE: A documented database using patterns and profiles as motif descriptors. *Brief Bioinform* **3**: 265–274.
- Sosa, O.A., Repeta, D.J., DeLong, E.F., Ashkezari, M.D., and Karl, D.M. (2019) Phosphate-limited ocean regions select for bacterial populations enriched in the carbon–phosphorus lyase pathway for phosphonate degradation. *Environmental Microbiology* **21**: 2402–2414.
- Souri, E., Kaboodari, A., Adib, N., and Amanlou, M. (2013) A New extractive spectrophotometric method for determination of rizatriptan dosage forms using bromocresol green. *DARU J Pharm Sci* **21**: 12.
- Studier, F.W., Daegelen, P., Lenski, R.E., Maslov, S., and Kim, J.F. (2009) Understanding the Differences between Genome Sequences of *Escherichia coli* B Strains REL606 and BL21(DE3) and Comparison of the *E. coli* B and K-12 Genomes. *Journal of Molecular Biology* **394**: 653–680.
- Suzek, B.E., Wang, Y., Huang, H., McGarvey, P.B., and Wu, C.H. (2015) UniRef clusters: a comprehensive and scalable alternative for improving sequence similarity searches. *Bioinformatics* **31**: 926–932.
- Thaller, M.C., Schippa, S., Bonci, A., Cresti, S., and Rossolini, G.M. (1997) Identification of the gene (*aphA*) encoding the class B acid phosphatase/phosphotransferase of *Escherichia coli* MG1655 and characterization of its product. *FEMS Microbiol Lett* **146**: 191–198.

- Thomashow, L.S., LeTourneau, M.K., Kwak, Y.-S., and Weller, D.M. (2018) The soil-borne legacy in the age of the holobiont. *Microbial Biotechnology* **12**: 51–54.
- Turner, B.L., Lambers, H., Condrón, L.M., Cramer, M.D., Leake, J.R., Richardson, A.E., and Smith, S.E. (2013) Soil microbial biomass and the fate of phosphorus during long-term ecosystem development. *Plant Soil* **367**: 225–234.
- U. Gandhi, N. and B. Chandra, S. (2012) A COMPARATIVE ANALYSIS OF THREE CLASSES OF BACTERIAL NON-SPECIFIC ACID PHOSPHATASES AND ARCHAEAL PHOSPHOESTERASES: EVOLUTIONARY PERSPECTIVE. *Acta Inform Med* **20**: 167–173.
- UniProt: a worldwide hub of protein knowledge (2019) *Nucleic Acids Res* **47**: D506–D515.
- Wang, Z., Tan, X., Lu, G., Liu, Y., Naidu, R., and He, W. (2018) Soil properties influence kinetics of soil acid phosphatase in response to arsenic toxicity. *Ecotoxicology and Environmental Safety* **147**: 266–274.
- Watt, G.D. (1990) A microcalorimetric procedure for evaluating the kinetic parameters of enzyme-catalyzed reactions: Kinetic measurements of the nitrogenase system. *Analytical Biochemistry* **187**: 141–146.
- Wickham H (2016). *ggplot2: Elegant Graphics for Data Analysis*. Springer-Verlag New York. ISBN 978-3-319-24277-4, <https://ggplot2.tidyverse.org>.
- Williams, B.A. and Toone, E.J. (1993) Calorimetric evaluation of enzyme kinetic parameters. *J Org Chem* **58**: 3507–3510.
- Zhang, G.-Q., Chen, Q.-J., Sun, J., Wang, H.-X., and Han, C.-H. (2013) Purification and characterization of a novel acid phosphatase from the split gill mushroom *Schizophyllum commune*. *Journal of Basic Microbiology* **53**: 868–875.

441

442

443

444

445

446 **Table 1: Strains and plasmids used in this study.**

447

448

Strains or plasmids	Genotype or relevant characteristics	Reference
<i>Escherichia coli</i> EPI 300	<i>recA1, endA1, araD139, rpsL, nupG, trfA</i>	Epicenter (Studier <i>et al.</i> , 2009)
<i>Escherichia coli</i> BL21(DE3)	F'/ <i>ompI, hsdS, gal, dam, met</i>	
Plasmids		
pMBL	Vector for cloning PCR amplicons, Ap	Dominion
pET28a	Expression vector, 6xHis, Km	Novagen
pET28::FOS M2-62	pET28 containing the complete gene encoding acid phosphatase FOSM 2-62	This study
pET28:BSU	pET28 containing the complete gene encoding acid phosphatase from <i>Bacillus subtilis</i>	This study
pET28:PYR	pET28 containing the complete gene encoding acid phosphatase from <i>Pyrococcus furiosus</i>	This study
pET28:MET_A1	pET28 containing the complete gene encoding the MEAT_A1 GAP acid phosphatase deduced from environmental metagenomes	This study
pET28:MET_A2	pET28 containing the complete gene encoding the MEAT_A2 GAP acid phosphatase deduced from environmental metagenomes	This study
pET28:MET_B1	pET28 containing the complete gene encoding the MEAT_B1 class B acid phosphatase deduced from environmental metagenomes	This study
pET28:MET_B2	pET28 containing the complete gene encoding the MEAT_B2 class B acid phosphatase deduced from environmental metagenomes	This study
pET28:MET_C1	pET28 containing the complete gene encoding the MEAT_C1 class C acid phosphatase deduced from environmental metagenomes	This study
pET28:MET_C2	pET28 containing the complete gene encoding the MEAT_C2 class C acid phosphatase deduced from environmental metagenomes	This study

449

450 Ap and Km stand for resistance to ampicillin and kanamycin.

451

452

453

454 **Table 2. Relative acid phosphatase activity of genes amplified from genomic DNA and**
455 **recovered from metagenomic libraries at different pHs.**

456

457

458

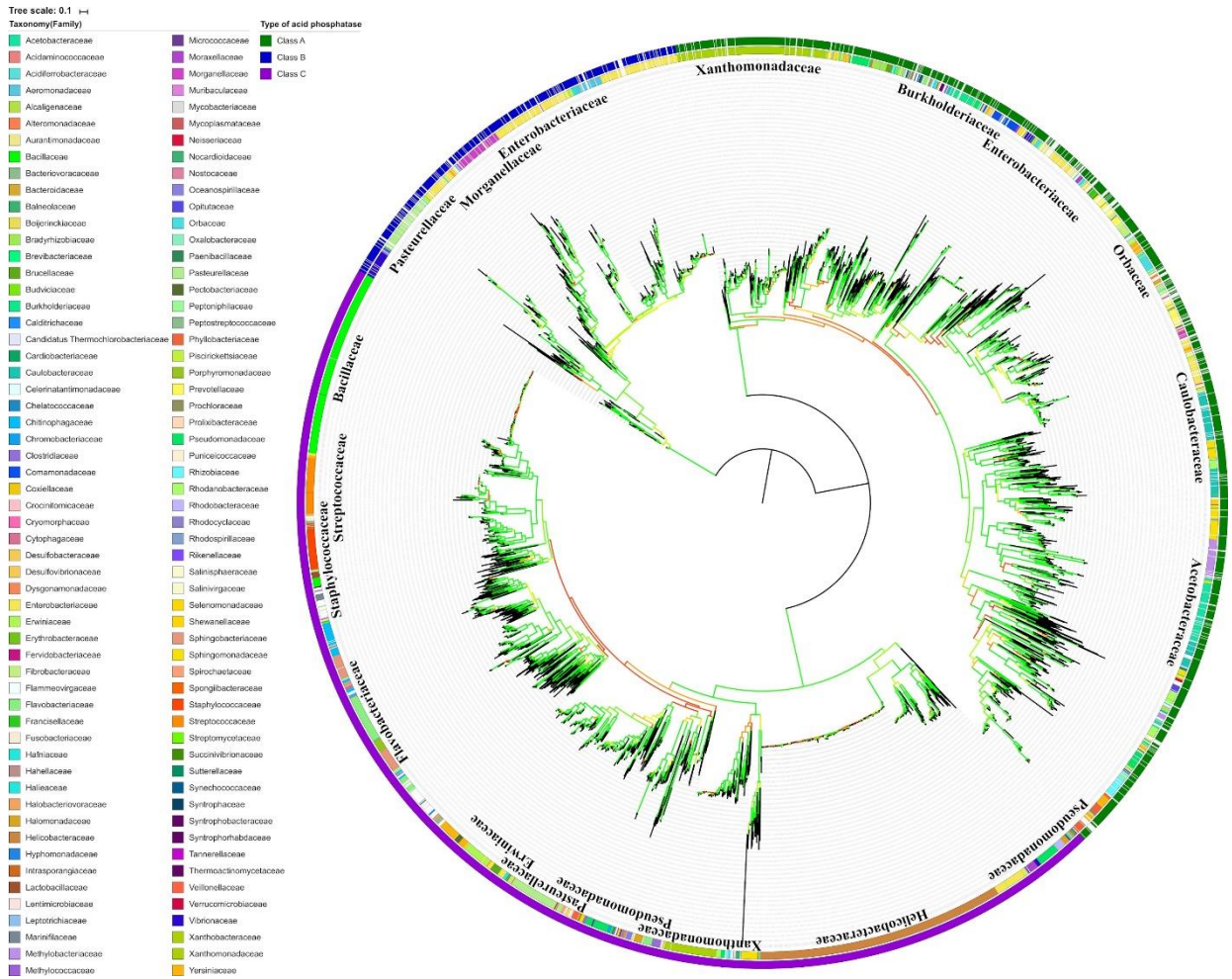
pH	Enzyme source							
	MET_A1	MET_A2	MET_B1	MET_B2	MET_C1	MET_2	M2-62	Bacillus
2	1	5	30	5	3	2	2	2
3	9	15	30	59	23	8	8	15
4	41	23	41	56	77	21	21	22
5	79	90	50	55	106	30	85	90
5.5	100	100	100	100	100	100	100	100
6	97	16	73	43	61	80	98	97
7	93	7	59	35	16	10	93	81
8	71	1	39	17	7	9	47	30
9	33	2	32	5	5	6	16	9

459

460

461 The set of acid phosphatases were expressed in *Escherichia coli* and the assays carried
462 out as described in Materials and Methods at different pH in Britton-Robisson poly-
463 buffer. Activities are expressed as relative activity, the maximum activity for all of the
464 enzymes was at pH 5.5 and the corresponding value is considered 100% in each case.
465 Results shown are the average of at least three replicates with standard deviations
466 below 20% of the given values. Supplementary Table 5 shows the activity for each
467 enzyme at pH 5.5 in nanomoles of *p*-nitrophenol produced per minute per milligram of
468 cell dry weight at 25°C.

469



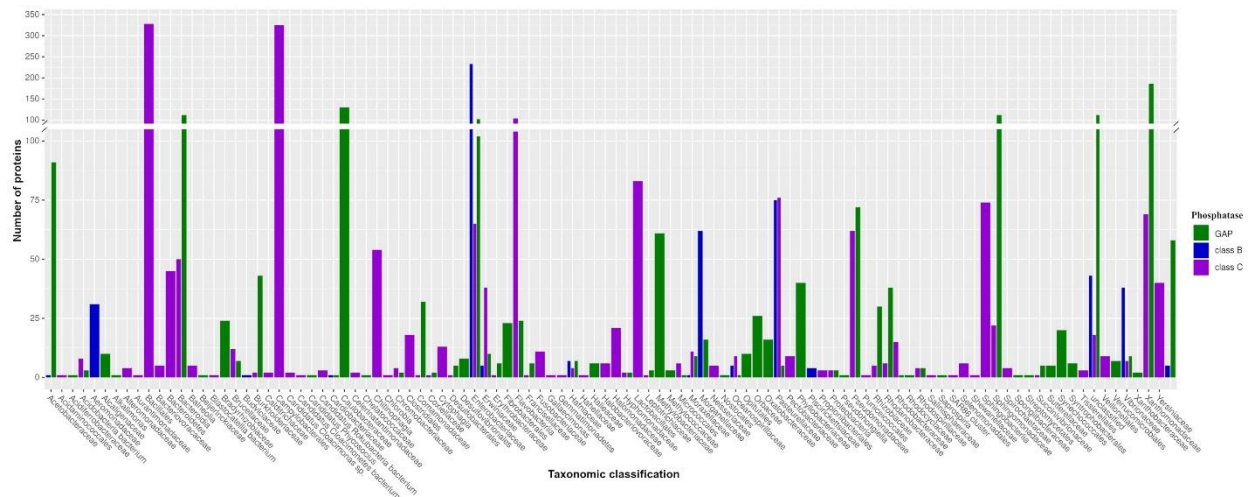
470

471

472

473 **Figure 1. Maximum likelihood phylogenetic tree of bacterial acid phosphatases.** The
 474 maximum likelihood tree was inferred from a simultaneous comparison of 3741 protein
 475 sequences of bacterial acid phosphatases. Tree topology and branch lengths were
 476 calculated by maximum likelihood using the WAG+F+R10 model of evolution for amino
 477 acid sequences in IQ-TREE software Nguyen et al., 2015. The tree was rooted by using
 478 clade B as an outgroup that shows a clear separation between the three clades of acid
 479 phosphatase proteins. Colours of the branches represent levels of significance obtained
 480 in the bootstrapping analysis using 1000 bootstrap replications. Green indicates
 481 percentages close to 100% of confidence in the bootstrapping analysis. The unrooted tree
 482 obtained using the same sample set it is shown in Supplementary Figure 1.

483



484

485

486 **Figure 2. Taxonomic distribution of the number of sequences used to construct the**
 487 **three acid phosphatase profiles (Prf-GAP, Prf-B and Prf-C).** Sequences were
 488 downloaded from the Uniprot database according to their functional annotation. The
 489 number of proteins per taxonomic group were plotted using ggplot2 library in R
 490 (Wickham et al., 2016).

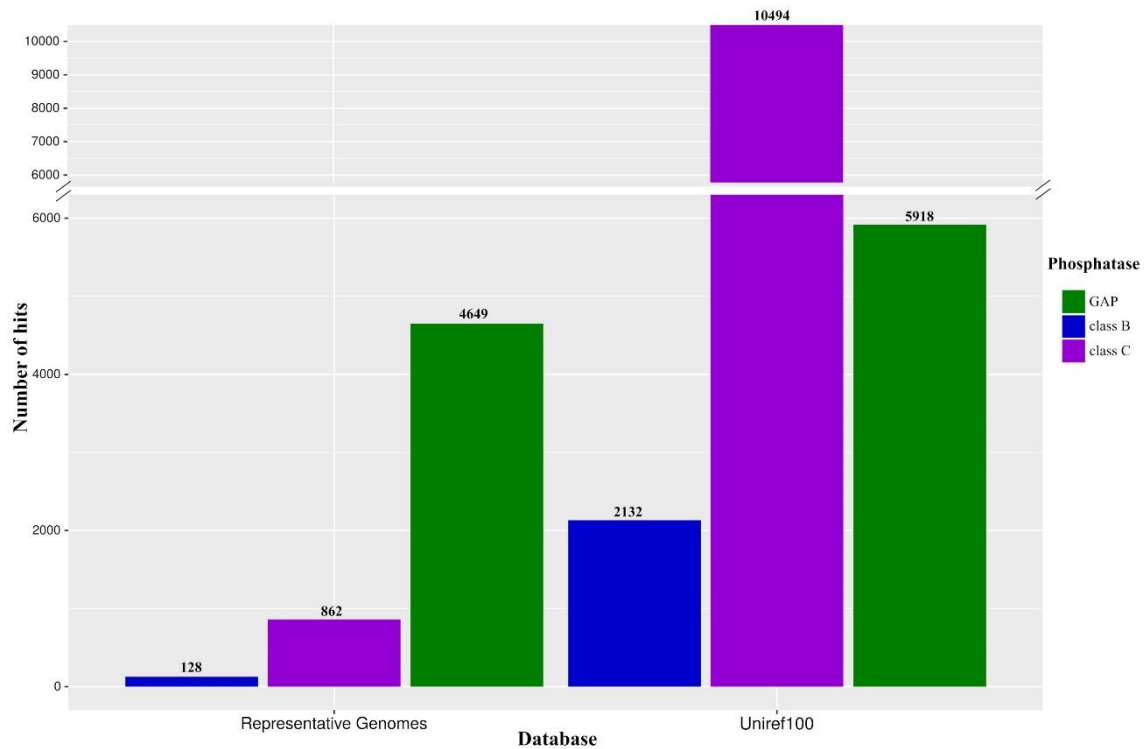
491

492

493

494

495



496

497

498 **Figure 3. Number of hits found by the constructed profiles of three classes of acid**
 499 **phosphatases (Prf-GAP, Prf-B and Prf-C).** Using *pfscan* tool on protein sequences from
 500 the Uniref100 database (the last three columns on the right) and a local database of
 501 proteomes of 5639 representative bacterial and archaea genomes (the three most left
 502 columns) downloaded from NCBI.

503

504

505 **SUPPLEMENTARY FIGURES AND TABLES.** They will provide upon request to Juan L.

506 **Ramos due to the large size of the files**

507

508

509

510